Vol. 39(2), pp. 144-164, Dec. 2020
ISSN 1821-536X (print)
ISSN 2619-8789 (electronic)

Tanzania Journal of Engineering and Technology

Full Length Research Paper

Assessment of the Performance of Grinding Circuit for Buzwagi Gold Mine

Alphonce Wikedzi

Department of Chemical and Mining Engineering, University of Dar es Salaam, Tanzania
Corresponding author: alpho20012001@gmail.com

ABSTRACT

It had been reported by the management of Buzwagi Gold Mine (BGM) that grinding circuit was designed to produce final product size of 125 µm, which had not been achieved for a long period of time under both, low to normal (i.e. 450-600 t/h) and high (i.e. > 650 t/h) throughputs. Also, the performance behaviour of the circuit had not been reviewed after long time of operation. Hence, an evaluation study was conducted in order to recommend improvement in mine operations. The study was realized through three circuit survey campaigns and laboratory experimentations. From the surveys, size distributions and solids contents of the samples were determined for all selected circuit streams. Furthermore, grindability and work indices of the ores were determined through standard Bond tests. The standard Bond tests data revealed increased Bond work indices for currently treated ores vs. those during design, indicating change in ore hardness over the years. Consequently, a periodic review of the ore blends was recommended as harder material requires more energy, which increases operation costs. Such reviews could help in establishing better ore blending and optimum throughput for existing plant design. Furthermore, the SAG mill circuit indicated varying feed sizes (i.e. $x_{F,80}$ =102 to 185 mm) which could be rectified by closer monitoring and control of ratios for the Semi-Autogenous Grinding (SAG) mill feeders drawing the ore from the stockpile. The ball mill performance was poor as indicated by only 5-9 % of < 125 µm (target product) in the discharge. This had a direct impact on hydrocyclones, where significantly poor performance indicators were observed; coarser overflow $x_{P,80}$: >200 µm as well as cut size, x_T: >200 µm. Also, the Bond efficiency factors in the range of 48-61 % were obtained, indicating an inefficient operation that could only achieve targets by lowering the current throughput. Hence, an optimization study of the existing design through computer modelling and simulation is recommended. Through simulation of multi-effects, a deeper understanding of the efficiency problems for the BGM grinding will be facilitated and also may provide possible solutions.

Keywords: *Comminution, Grinding circuit, SAG mill, Ball mill, Circuit survey, Bond work index, Bond efficiency factor, Gold ore blends.*

INTRODUCTION

Comminution is one of the most important unit operations in mineral processing and chemical industry (Denız, 2011; Fuerstenau *et al*., 2011). However, comminution processes are both energy-intensive and expensive, with tremendous

room for improvement. It is estimated that comminution accounts for up to 50% of the energy used in mining operations (Ballantyne *et al*., 2012; Boucaut, 2017; Curry *et al*., 2014; Jeswiet and Szekeres, 2016) and that only 1% to 2% of the supplied energy is effectively translated in the creation of new surface areas (Rosario, 2010; Tromans, 2008; Wills and Finch, 2016). The majority of this energy is lost as heat or mechanical energy due to the operating nature of mills, where energy transfer between grinding media and particles is unconstrained and completely random.

This expensive and inefficient comminution process also represents a significant fraction of the global electric power consumption. In the United States, it is estimated that 30% of the total energy costs consumed in mining industry goes for comminution processes (DOE indices for 2005) (NRC, 1981; Tromans, 2008). Thus, comminution energy makes around 0.39% of total national energy consumption. In Canada, in turn, the respective index comes to nearly 2%, similarly in the Republic of South Africa. In Australia comminution consumes roughly 1.5% of total national energy (Tromans, 2008). It has to be noted that, USA, Canada, South Africa, and Australia are the leaders in the application of modern mining technology and in recent years the values of energy consumption indices have generally decreased as a result of the application of modern processing technologies and equipment, especially in ore preparation circuits. As a result of the above, it is estimated that industrial comminution processes can absorb from 3 to 5% of global electric energy consumption (Jeswiet and Szekeres, 2016; Saramak *et al*., 2010). These and many other statistics reveal the importance and impact of size reduction processes and the reason for the extensive amount of effort made on this subject over the last 50 years (Acar, 2013).

In recent years, there have been significant developments in comminution efficiency, both due to the expansion of machines with the capability to boost energy utilization, and also due to optimal design of grinding circuits and operating variables that enable more efficient application of existing machines (Vedat, 2011). However, as a consequence of depleting high-grade ores; the mining industry's future trends indicate that the need will continue to mine and treat low grade, finely disseminated ores at much higher tonnages and finer product size. The effective liberation of valuables from such ores remains one of the major challenges for the mining industry (Danha, 2013).

The combination of energy intensive and poor performance of comminution process implies that there is a great opportunity for significant energy and economic savings by the improvement of this process (Rosario, 2010). Even small improvements to the power utilization efficiency can have a significant influence on the economic performance of a plant. Hence, continued research and development that will contribute to continued efforts in improving these processes is necessary for the long-term viability of the mining industry.

Previous work by Wikedzi (2018) concentrated on grinding circuit performance, with the case of Buzwagi Gold Mine (BGM). The survey data collected at BGM plant between April and June 2015 indicated clearly that, by then, BGM grinding circuit was designed to produce final product size of 125 µm, which had not been achieved under both, low to normal (i.e. 450-600 t/h) and high (i.e. > 650 t/h) throughputs (Figure 1). It was also reported that the performance behavior of the circuit had not been reviewed after long time of operation. Such a situation was anticipated to have not only lowered the flotation

performance, but also limited the state-of-the-art data on the overall performance of the process plant.

Therefore, any effort aimed at improving the performance of the operation became necessary. This could be achieved through several full-scale plant surveys in order to analyze the state-of-the-art performance of the circuit as well as investigate and improve ore breakage and grindability properties through feed ore characterization. Furthermore, based on analysis of the survey data and feed ore characterization tests, circuit optimization opportunities could be identified and implemented. As BGM operations are close to an end, the study will help other mining operations with similar problem.

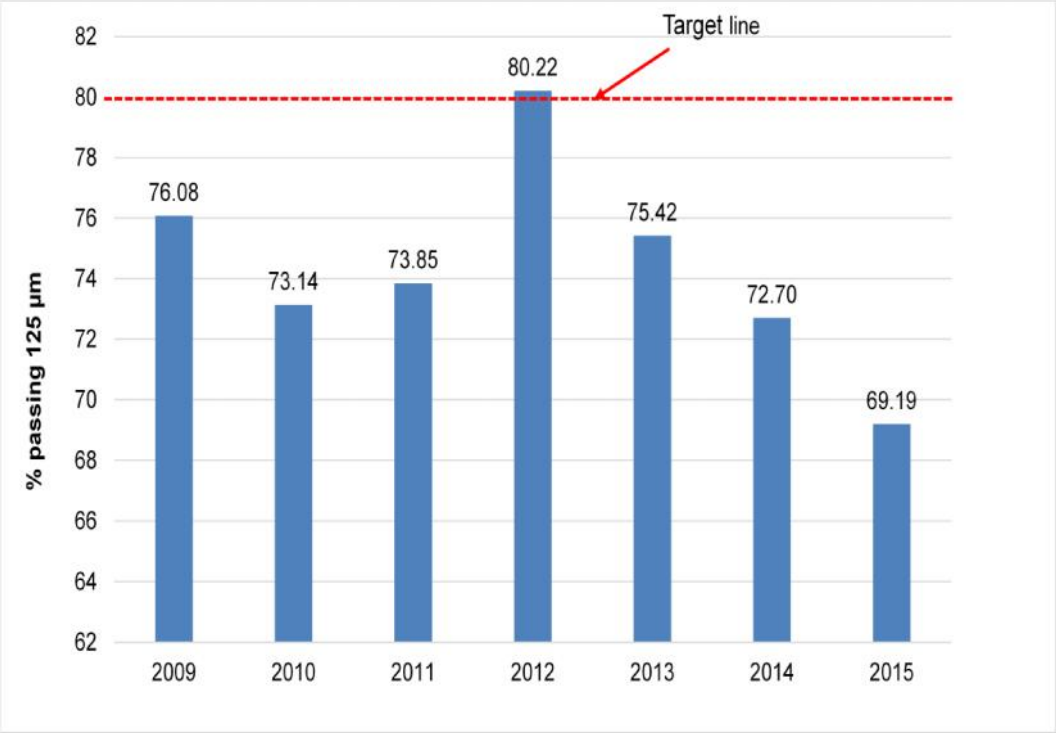

Figure 1: BGM grinding circuit efficiency trends from 2009 to 2015

THEORY

Grinding Circuits Efficiency

The most applicable technique in determining the efficiency of comminution circuits is the use of Bond efficiency factor (B_{ef}), which is the relative efficiency of the grinding circuit compared to the prescribed Bond standard energy for a 'conventional' grinding circuit (Rowland, 2008). The Bond efficiency factor is calculated as shown in equation (1).

$$B_{ef} = \frac{W_i}{W_{i,op}} \quad \text{.....(1)}$$

Where B_{ef}, W_i, and $W_{i,op}$ are Bond efficiency factor (%), laboratory Bond index (kWh/t) and operating Bond work index (kWh/t), respectively. Efficiency factor values larger than 100 % imply that the mill consumes less energy than the laboratory Bond tests estimate, and thus the throughput can be increased. On the contrary, efficiency values of less than 100 % imply that the milling operation is inefficient and energy is wasted by the

grinding operation (Alamouti *et al*., 2011; Rowland, 2008). The operating Bond index, $W_{i,op,}$ can be determined from survey data by equation (2).

$$W_{i,op} = \frac{P}{\dot{m}\left(\frac{10}{\sqrt{x_{P,80}}} - \frac{10}{\sqrt{x_{F,80}}}\right)} \quad \ldots\ldots\ldots (2)$$

Where P is the circuit power in kW, $\dot{m}$ is circuit throughput (t/h) and $x_{P,80}$ and $x_{F,80}$ are the circuit product and feed sizes, respectively.

The laboratory work index is obtained using the standard Bond test procedure and using Bond (Equation (8). This parameter is used for estimation of specific power requirements for industrial grinding mills (Rowland, 2006). The operating work index is the specific power consumption under real plant conditions based on known mill throughput, power draw and size distributions of feed and product. It is regularly used for monitoring energy efficiency of existing grinding circuits (Gupta and Yan, 2006; Napier-Munn *et al*., 1996; Rowland, 2006).

Performance of Classification Processes

It is a normal practice for most grinding circuits to be incorporated with classification devices (e.g. screens or hydrocyclones) which their main function is to remove the already ground material to the next unit operations. This step is important, otherwise, overgrinding can occur and cause unnecessary energy costs as well as metal losses. Ideally there is no technical classifier which can achieve 100% separation of the feed into a stream of fines only and another stream of coarse particles only at a defined cut size. Due to stochastic factors of particle collisions, turbulence and flow pattern within the separating medium some of the fine particles will report to the coarse stream and also some of the coarse particles will report to the stream of fine particles (Khumalo, 2007; Schubert, 1985; Schubert and Mühle, 1991).

The efficiency of classification devices like screens and hydrocyclones is typically presented by the so called partition curve T(x) (Figure 2), also known as performance curve (Gupta and Yan, 2006; Leißner *et al*., 2016; Schubert, 2003; Wills *et al*., 2006). The partition curve relates the weight fraction of each individual particle size which reports to the apex (also called underflow or coarse product stream), to the weight fraction of the same particle size in the feed. From the curve, the cut size x_T is defined as the size for which 50 % of the particles in the feed report to the coarse product stream. Particles of this size have an equal chance of going either to the overflow or underflow stream.

It is worth to note that T(x) does not pass through the origin due to the fact that, a fraction of particles bypasses the classifier and are not classified (Gupta and Yan, 2006), which is especially relevant for all (hydro-) dynamic classifiers. Thus, the cut size calculated from T(x) has to be corrected in order to account for the bypass effect.

The usual symbol for the corrected cut size is x'_T. The following equations are involved in the assessment of a given classifier:

$$T(x) = (1 - R_{m,f})\frac{m_C(x)}{m_F(x)} \quad \ldots\ldots\ldots\ldots (3)$$

Where: $R_{m,f}$ = Fraction of particles recovered in the fine product stream; m_C(x) = weight fraction of particle size x in the coarser product stream; m_F(x) = weight fraction of particle size x in the feed stream

$$T'(x) = \frac{T(x) - T_o}{1 - T_o} \quad \ldots\ldots\ldots\ldots\ldots\ldots (4)$$

$$x'_T = T(x'_T) = 0.5 \quad \ldots\ldots\ldots\ldots\ldots (5)$$

where T_o = the splitting factor.

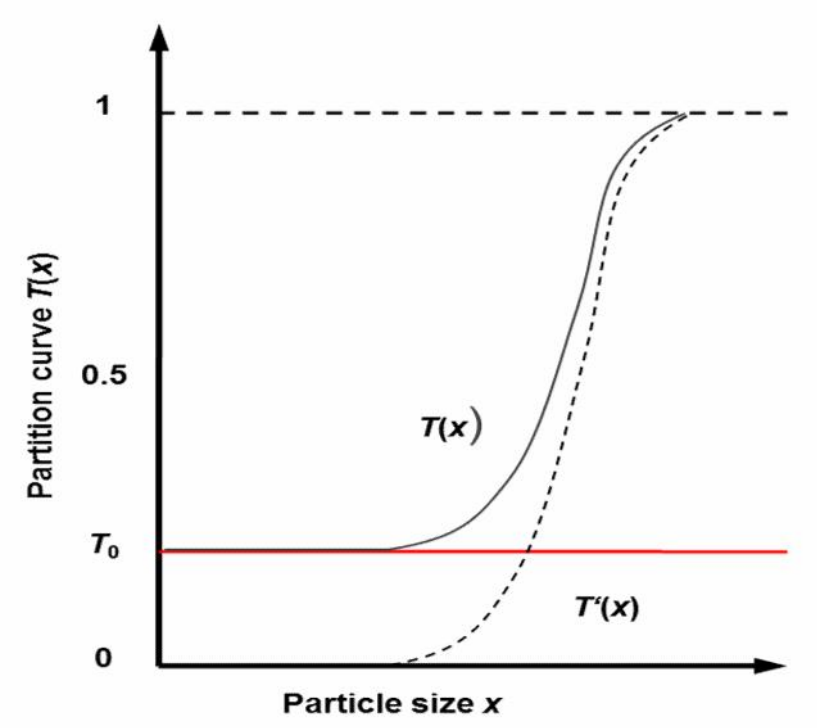

Figure 2: Typical partition curve for hydrocyclones

The sharpness of the cut is represented by the slope of the central section of the partition curve; the closer to vertical is the slope, the higher is the efficiency. The imperfection (*I*) as well as efficiency of separation (©) are given by equations (6) and (7), respectively:

$$I = \frac{x_{75} - x_{25}}{2x_{50}} \quad \ldots\ldots\ldots\ldots\ldots\ldots (6)$$

$$© = \frac{x_{25}}{x_{75}} \quad \ldots\ldots\ldots\ldots\ldots\ldots\ldots\ldots (7)$$

x_{25} and x_{75} are sizes at which 25 % and 75 % of the feed particles report to the coarse stream.

MATERIAL AND METHODS

BGM grinding Circuit Survey

Comminution circuit survey is an essential tool for gaining an understanding of grinding operations over a particular time period. It involves collection of representative samples and operating data from the circuit over a particular operating period. However, a good survey has to be conducted based on the standard survey procedures and protocol as proposed by Napier-Munn and co-workers (Mular *et al*., 2002; Napier-Munn *et al*., 1996), which were also implemented in the current study.

For the purpose of this study, three full scale sampling survey campaigns, each lasting for a maximum period of 2 hours were implemented on the BGM grinding circuit. Prior to sampling, circuit operating conditions were monitored to ensure that the plant is under steady state conditions. This was verified by examining the real time circuit trends for the key circuit parameters from the control system for at least 2 hours.

The sampling and steady state monitoring points used for BGM grinding circuit are shown in Figure 3 and the respective samples collected are listed as follows:

1) SAG mill feed
2) SAG discharge screen undersize
3) Pebble crusher feed

4) Pebble crusher product
5) Cyclone feed
6) Cyclone underflow
7) Cyclone overflow
8) Ball mill discharge

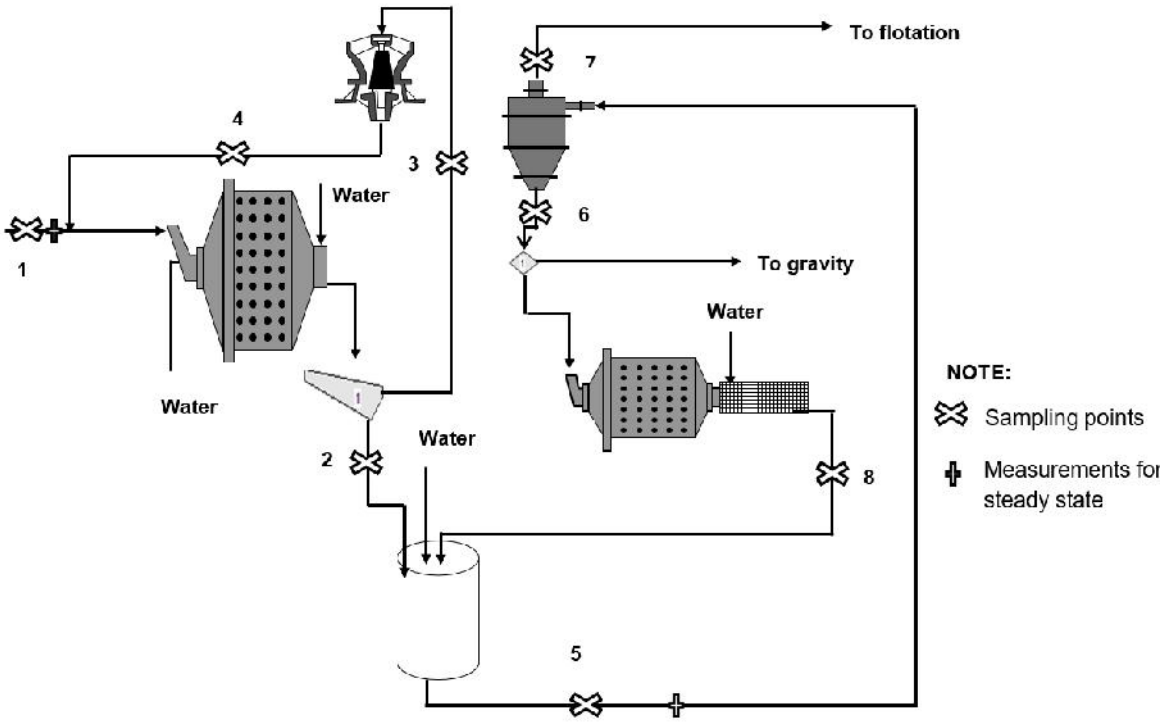

Figure 3: BGM grinding circuit flow sheet with sampling points.

Based on the design of the circuit, it was not possible to sample the SAG mill discharge. The flow rate for this stream was later determined from the mass balance of the other streams sampled. Also, it has to be realized that samples 1, 3 and 4 are mainly solids, while the rest are slurry. These two categories of samples were obtained as follows.

SAG Mill Feed sampling

The Semi-Autogenous Grinding (SAG) mill feed sample was obtained by stopping the circuit feed conveyor and then stripping the ore (belt cut sampling). The stripped conveyor length was 3-4 m. The quantities of the SAG feed samples collected were approx. 377.5, 341.2 and 315 kg, for sampling survey campaign 1, 2 and 3, respectively.

Pebble Crusher Feed and Product sampling

In each survey, the pebble crusher feed sample was grabbed from the pebble crusher feed diverter chute after every 20 minutes interval by the aid of a shovel. Pebble crusher product samples were obtained from the pebble crusher product discharge chute using the same time interval, procedure, and device as for the feed. The quantities of samples collected for the pebble crusher streams for each survey are presented in Table 1.

Table 1: Total mass of samples collected for pebble crusher streams.

Stream Name	Surveys		
	S-1	S-2	S-3
Pebble crusher feed in kg	27.74	33.45	40.42
Pebble crusher product in kg	16.70	26.00	24.00

Sampling Slurry Streams

Slurry sampling was done for the undersize material of the SAG discharge screen, the cyclone feed, overflow, and underflow as well as the ball mill discharge. During the whole campaign, each slurry stream was sampled every 15 minutes for a period of two hours. A total of 8 subsamples were collected to make the composite weight (i.e. Table 2) for the final sample. This was done in order to reduce possible sampling error due to operation or process fluctuations (i.e. plant dynamics). However, the other possible source of errors could be due to sample cutter design, sub-sampling (e.g. splitting) of primary sample, analytical errors (e.g. weighing, inadequate sieving time, etc.) as well as propagation errors due to calculation of quantities (e.g. solids concentration).

Table 2: Slurry streams composite sample weights collected.

Stream/sample name	Survey		
	S-1	S-2	S-3
SAG discharge screen undersize in kg	18.12	20.04	20.30
Ball mill product in kg	7.15	20.30	20.80
Cyclone feed in kg	14.22	17.66	20.83
Cyclone underflow in kg	15.60	10.40	12.50
Cyclone overflow in kg	6.60	7.80	9.90

Napier-Munn and co-workers (Napier-Munn *et al*., 1996) recommends the range of sample mass required for a representativeness of the survey campaign. All samples collected in this case were within this recommendation. In all of the proceeding sections, the notation S-1, S-2 and S-3 will be used to refer to survey 1, survey 2 and survey 3 samples, respectively.

Other Data Collected

To successfully assess any grinding circuit, apart from material sampling exercise, also design and existing operating parameters of the circuit are required. Design parameters were obtained from the design documents and include equipment specification, equipment type and operating conditions. Current operating parameters were recorded from the control system and comprise of plant feed rate, grinding mills power draw, weight, water addition rate, speed as well as cyclone pressure. The mill ball load was determined by measuring the free height between balls load and the mill shell (Gupta and Yan, 2006; Napier-Munn *et al*., 1996) during plant breakdown, which occurred a day before survey. The details of the design parameters collected during the three full survey campaigns for the BGM grinding circuit are presented in Table 3.

Processing of Samples

All samples collected around the grinding circuit were dried and sieved in order to determine the solids content and particle size distributions. Slurry samples and pebble crusher samples were treated onsite, while the SAG mill feed samples were transported and processed at the Institute of Mechanical Process Engineering and Mineral Processing, TU Bergakademie Freiberg in Germany. Apart from particle size analysis, SAG mill feed samples were also used for standard Bond tests in order to determine ore grindability and work indices.

Table 3: Summary of design criteria for BGM grinding circuit

Design parameter	SAG Mill	Pebble Crusher	Ball Mill	Hydro-cyclone
Feed rate in t/h	460-543	190		1462
Feed $x_{F,80}$ in mm	120			
Power in kW	6000	315	6000	
Ball charge in % volume	15-20		30-35	
Total charge in % volume	30-35			
Critical speed in %	75		75	
Ball size in mm	65/90/120/150		80/65/50	
CSS in mm		10-14		
Final product $x_{P,80}$ in µm			125	
Bond Ball Mill Work Index in kWh/t			11.6-14.8	
Bond Rod Mill Work Index in kWh/t			15.3-16.5	
Pressure in kPa				80-110
Circulating load in %				250-350
Overflow product $x_{P,80}$ in µm				100-125

Particle Size Analysis

The dried slurry samples used for percent solids determination were also used for particle size analysis. The sieving process and equipment/devices involved for all samples is well summarized in Table 4.

The Standard Bond Test

The three SAG mill feed samples (S-1, S-2, and S-3) obtained from the belt cut of the feed conveyor were used for determination of their respective work indices. To obtain materials which are suitable for the standard Bond test, representative sub-samples were prepared from the bulk samples by stage laboratory crushing (jaw and cone crushers) to produce < 5 mm material, followed by splitting (riffle splitter). The standard Bond feed material (< 3.15 mm) were obtained after further crushing with a laboratory jaw crusher. This general sample preparation procedure is shown in Figure 4.

Bond developed standard laboratory tests for the determination of crushability and grindability indices (Bond, 1952) and later modified it (Bond, 1961). The indices are the measure of material's resistance to breakage and are applicable in his empirical energy-size-reduction model to estimate the energy requirement in comminution (Masuda *et al*., 2007).

The standard Bond's test is a batch type dry test where the mill is operated in a locked cycle. The charge is ground for a number of mill revolutions, sieved on the desired screen to remove undersized material and then replacing the undersized material with new feed. The procedure is repeated until a constant mass ratio of 2.5 for oversize and undersize is achieved for three consecutive cycles (i.e. equilibrium condition). Mosher and co-worker (Mosher and Tague, 2001) found that the minimum number of cycles for the Bond test is seven, no matter how fast the steady state conditions are achieved.

Table 4: Particle size analysis procedure for the survey samples.

Sample	Procedure	Device/Equipment used
SAG mill feed	- Whole bulk sample used - >45 mm: Manual sieving - <45 mm: analytical sieving machine	- 450 mm sieves - Sieve series in mm: 200, 150, 125, 90, 63, 45,31.5, 25, 20, 16, 12.5, 10
Pebble crusher feed	whole weight of dried sample was used	- 450 mm sieves - Sieve series in mm: 50, 37.5, 26.5, 19, 13.2, 9.5
Pebble crusher product		- 450 mm sieves - Sieve series in mm: 26.5, 19, 13.2, 9.5, 6.7, 4.75, 3.35, 2.36
Hydrocyclone feed	- Splitting dried samples to obtain representative subsample	- Riffle splitter - 200 mm sieves - Sieve series in mm: 4.75, 3.35, 2.36, 1.7, 1.18, 0.85, 0.6, 0.425, 0.3, 0.212, 0.15, 0.106
Hydrocyclone underflow		
Ball mill discharge		
Hydrocyclone overflow		- Riffle splitter - 200 mm sieves - Sieve series in mm: 0.425, 0.3, 0.212, 0.15, 0.106, 0.075, 0.063

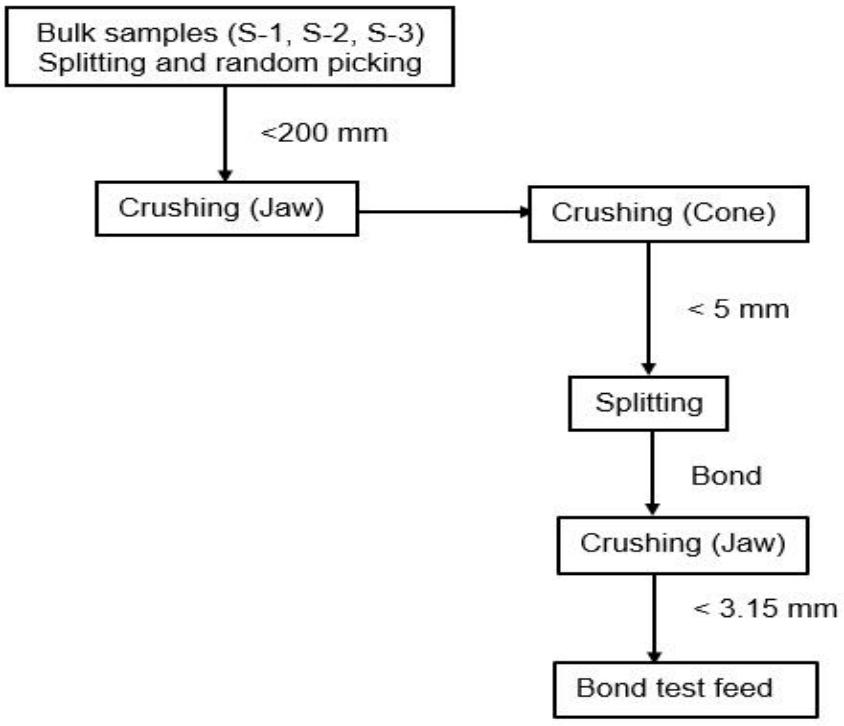

Figure 4: Overall preliminary sample preparation steps for the major tests

In this study, the standard Bond test protocols were adopted and the complete description of the test may be found elsewhere (Bond and Maxson, 1943; Magdalinović, 1989; Man, 2002). The closing screen used for the investigation is 90 µm. The test gives the standard work

index (W_i), which is calculated from Equation (8).

$$W_i = \frac{44.5}{P_1^{0.23} \cdot G_{bp}^{0.82} \cdot \left(\frac{10}{\sqrt{x_{P,80}}} - \frac{10}{\sqrt{x_{F,80}}} \right)} \quad \ldots\ldots\ldots\ldots\ldots\ldots\ldots\ldots\ldots\ldots\ldots\ldots (8)$$

Where $x_{F,80}$ and $x_{P,80}$ are 80%-passing size (µm) of feed and product, respectively, P_1 is the test sieve size used (µm), and G_{bp} is the net grams of sieve undersize material produced per mill revolution. Since Bond had used short tons to determine the work index equation (8), has to be multiplied by a factor of 1.1 in order to convert to metric tonnes. The work index of the material for the present work was calculated as an average of three tests conducted for each bulk sample. In this case, a 30.5 by 30.5 cm, standard Bond mill was used for the dry tests. The mill design and operating variables for the mill are presented in Table 5. Moreover, the analysis of particle size distributions as well as work indices data were conducted by using excel.

Table 5: The standard Bond mill operating parameters used for the tests.

Mill	Inner diameter	mm	305
	Length	mm	305
	Volume	cm³	22273
Mill speed	Critical speed	rpm	79.94
	Operational speed	rpm	70.00 (· := 85%)
Balls	Material		alloy steel balls
	Diameter	mm	19, 25, 38
	Specific gravity	g/cm³	7.81
	Number of balls		43 balls Ø 38 mm
			109 balls Ø 25 mm
			143 balls Ø 19 mm
	Total mass	kg	20.55 kg
Material	Gold ore		
	Specific gravity	g/cm³	2.8
	Total material filling	ml	700.00

RESULTS AND DISCUSSION

Grindability Studies

The work index for the Buzwagi ore deposit estimated during the plant design was in the range of 14.5 to 16.5 kWh/t. The currently treated ore blend's work indices (Table 6) ranged from 17.20 to 18.67 kWh/t. These higher work indices indicate a change in hardness of the ore during the last 7 years.

Overall, higher work indices have a negative impact on the energy costs of milling. Also, as the mining progresses, new parts of the deposit may be discovered, which may have different characteristics from the original plant design. This situation requires a periodic re-assessment of the grindability and work indices of the different ore types encountered which was not done by BGM since plant commissioning. The indicated change in ore hardness is in agreement with studies by Abbey and co-workers (Abbey *et al*., 2015) who investigated the impact of mining depth on the ore work index and found that the competence of the ore and work indices increase with increasing mining depth.

Table 6: Ore work indices during design vs. the current operation (survey results)

Survey	Measured (kWh/t)	Design (kWh/t)
S-1	17.20 ± 0.15	14.50 – 16.5
S-2	18.67± 0.05	
S-3	18.47± 0.2	

Grinding Circuit Mass Balance

Table 7 shows the mass balance for key streams in the circuit. In all surveys, the throughput was higher up to 22% than the design capacity. Additionally, the designed circulating load of 250-350% is slightly lower than the average value found during the three surveys (375%). This implies that the circuit was overloaded. Moreover, the SAG mill dilution ratio was higher for survey 1 (0.54) compared to survey 2 (0.45) and survey 3 (0.37). It is reported that the pulp density should be as high as possible so that the grinding media is coated with a layer of ore. If the pulp is too dilute, a metal to metal contact increases giving increased steel consumption and reduced grinding efficiency (Schlanz, 1987).

The fraction < 125 µm (target size) in the ball mill product is considered as an indicator for the efficiency of the grinding stage. The results show that this fraction was only between 5 to 9%. This poor performance might be due to the high circulating load of the ball mill circuit, which reduces the residence time of the material in the mill and hence leads to a coarser product.

SAG Mill Circuit

According to Figure 3, the Semi-Autogeneous Grinding (SAG) mill at BGM is in closed circuit with a pebble crusher. The performance of the pebble crusher is indicated by the particle size distribution of feed and product streams (see Figure 5). The differences in product fineness for the three surveys has a direct relationship with pebble crusher throughput and ore hardness (i.e. the higher the throughput, the coarse the product and vice versa). Therefore, survey 1 (i.e. 61 t/h) with the lowest throughput gave the finest product ($x_{P,80}$ = 20 mm) than the other two surveys with 70 t/h ($x_{P,80}$ = 23 mm) and 68 t/h ($x_{P,80}$ = 34 mm), respectively. Furthermore, the feed for surveys 2 and 3 were harder ore types than for survey 1 (see Table 6). When the feed becomes harder, the rate of breakage in the SAG mill decreases, leading to higher proportion of critical size product (pebbles), resulting to increased recycle load as reflected in the result (Pourghahramani, 2012).

Also, as it was expected, the product size ($x_{P,80}$) correlates with the operating gap of the crusher (Table 8). However, it has to be noted that the crusher feed rate for all three surveys was significantly lower than the design capacity of 190 t/h, implying that this equipment presents a reserve capacity. Further, it was observed that the feed and product size distributions for S-3 are quite close to each other. This indicates low reduction ratio of the pebble crusher, which could be due to the large operating gap (closed side setting).

Figure 6 and Table 9 present the particle size distributions and key performance indicators for the SAG mill, respectively. The SAG mill average feed size (Table 9) for survey 1 (185 mm) was significantly higher compared to surveys 2 (102 mm) and 3 (122 mm). The reason for this might be due to unmonitored gap of the primary crusher or feeder proportions from the stockpile. Since the design feed size for the SAG mill was 120 mm, this higher feed size will have contributed to the poor grinding performance in survey 1.

The hardness of the ore is an important parameter for SAG mill efficiency. Literature reports that, in SAG mills, soft ores are is mainly ground by impact breakage while hard ores are subjected to

abrasion and attrition events where the media impact could not sufficiently break harder particles (Pourghahramani, 2012).

Table 7: BGM grinding circuit performance indicators as recorded/calculated during survey.

Stream/Unit name	Survey			Target/Design
	S-1	S-2	S-3	
SAG Mill				
Throughput (t/h)	618.72	674.11	573.35	543-566
Power draw (kW)	5387	6147	6198	6000
Dilution ratio	0.54	0.45	0.37	
Ball Mill				
Discharge (t/h)	1109.91	939.83	487.42	
Power draw (kW)	5294	5399	5230	6,000
%< 125 µm	7.40	9.23	4.65	80
Hydrocyclone				
Feed (t/h)	1729.04	1613.93	1060.74	1462
Underflow (t/h)	1387.48	1249.57	840.08	
Overflow (t/h)	341.82	363.90	220.66	
Circulating load, *CL* (%)	400.00	344.00	381.00	250-350

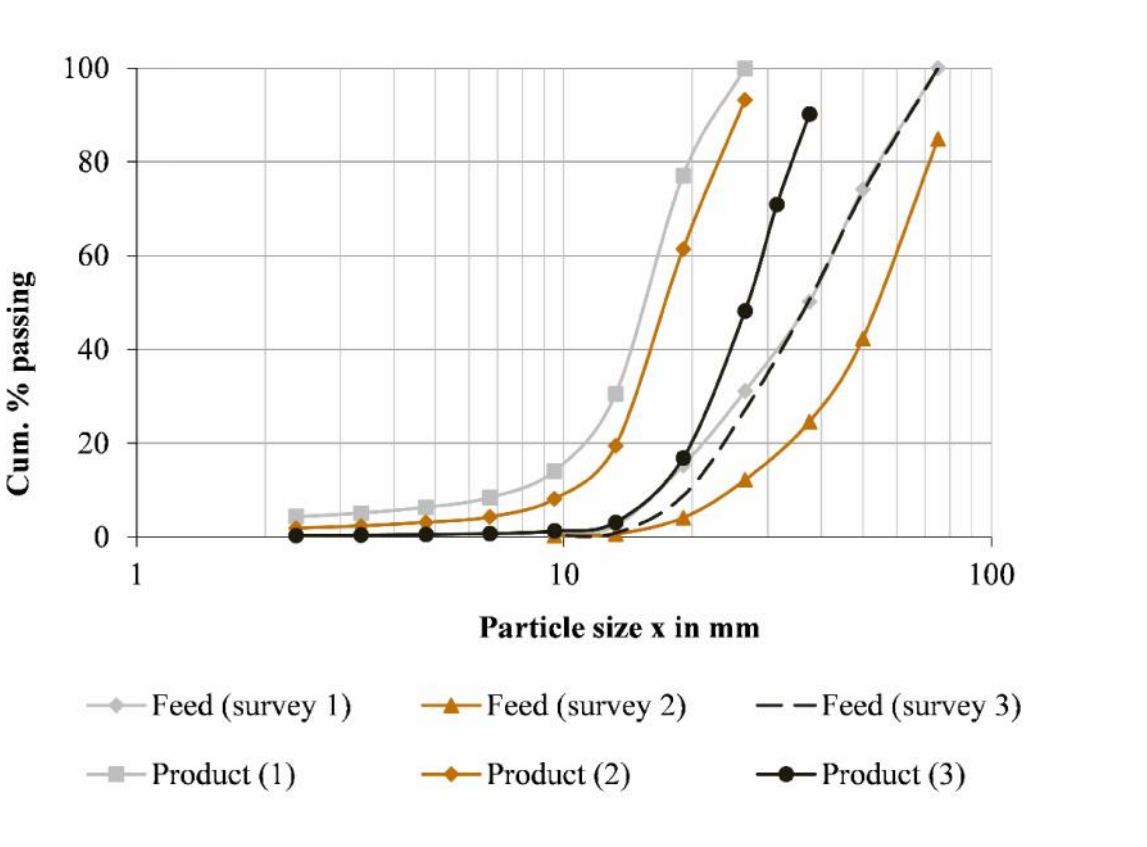

Figure 5: Pebble crusher streams particle size distribution

Table 8: Pebble crusher performance indicators.

Parameter	S-1	S-2	S-3	Design
CSS (mm)	12	13	20	14/10
Feed (t/h)	61.01	70.45	68.53	190
$x_{F,80}$ (mm)	56	72	56	
$x_{P,80}$ (mm)	20	23	34	

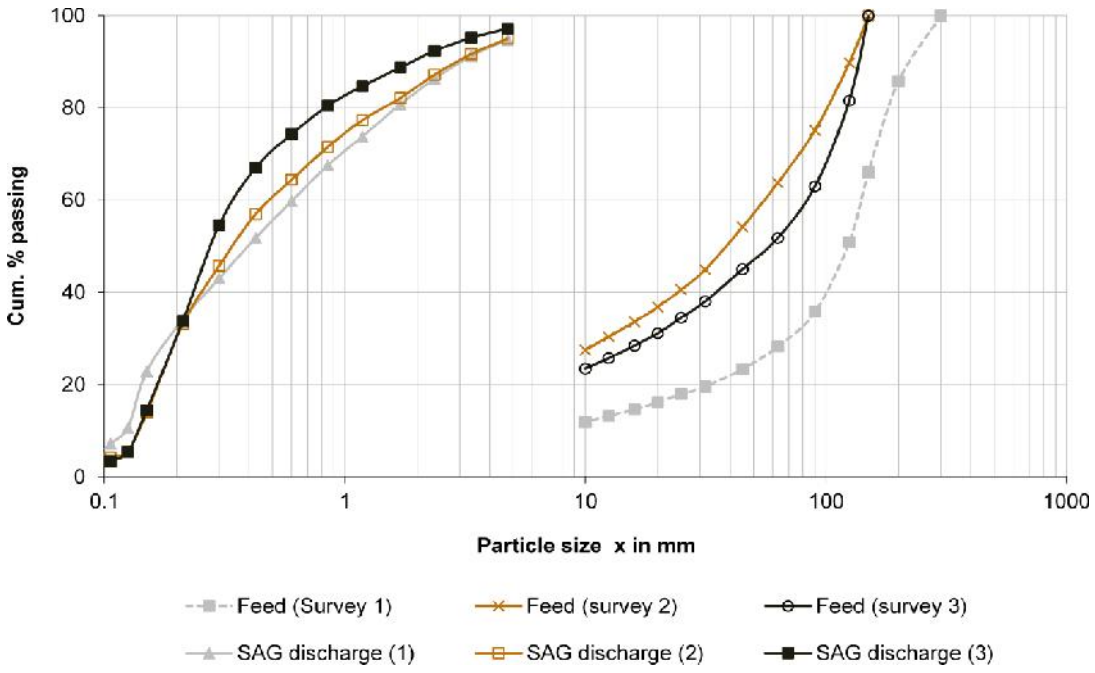

Figure 6: **SAG mill feed and product particle size distribution for survey 1, 2 and 3**

This can be reflected in this study, whereby, the harder the feed (Table 6), the finer the SAG mill product (Table 9). This had also an influence on the overall circuit product size (i.e. ball mill product). It can further be observed that, SAG mill products size was influenced by the specific energy. The higher the energy input employed, the finer becomes the final product size and vice versa as could be expected. Moreover, the reduction ratios achieved by the SAG mill were within recommendation.

The observed fluctuation in SAG mill feed size is a problem that needs to be addressed. Regular monitoring and control of the SAG feed size is important as the change in feed size distribution normally results to corresponding changes in the grinding media size distribution, which has further impact on power and throughput (Napier-Munn *et al.*, 1996; Wills *et al.*, 2006). This could be achieved through regular monitoring of the primary crusher performance through analysis of the product size distribution. Since the SAG mill is fed by the ore drawn from the stockpile through three feeders, the SAG mill feed size distribution could also be influenced by the proportion or ratios at which the feeders draw the ore. Hence, closer control of the feeders is also important.

Table 9: SAG mill performance indicators.

Parameter	S-1	S-2	S-3	Design
SAG mill feed rate (t/h)	618.72	674.11	573.35	543-566
SAG mill feed, $x_{F,80}$ (mm)	185.45	101.6	122	120
SAG discharge $x_{P,80}$ (mm)	1.644	1.468	0.831	
SAG mill reduction ratio (-)	113	69	147	
SAG mill specific energy (kWh/t)	7.92	8.26	9.47	
Ball load, % volume	14.30	14.30	-	15-20
Material load, % volume	20	20	-	30-35

Ball Mill Circuit

The particle size distribution of ball mill streams is presented in Figure 7. Little can be seen in terms of differences in the ball mill performance for the three surveys. Based on the product fineness and reduction ratios (Table 12), it can be seen that the ball mill operation was inefficient. The poor performance might have been due to higher circulating load (Table 7) and coarser SAG mill discharge (Table 9)experienced by the operation. Further, the efficiency of the ball mill is seen to depend on the input energy as well as the circuit throughput (Table 7).

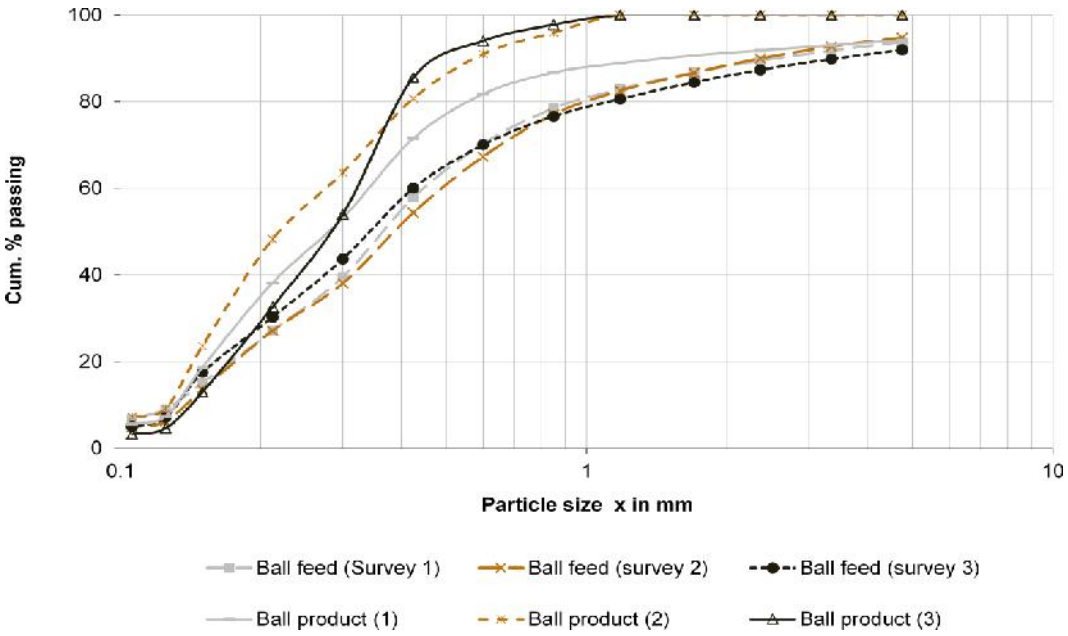

Figure 7: **Ball mill feed and product particle size distribution for survey 1, 2 and 3**

Figure 8 to Figure 11 and Table 11 to Table 13 present the results for the size distributions and some key performance indicators, respectively, for the BGM hydrocyclones obtained during the three surveys. The result shows that the overflow product size ($x_{P,80}$) is much coarser than target (i.e. 125 µm) in all surveys (Table 11). Since the ball mill products were significantly coarser than once designed, the coarse overflow achieved could also be contributed by the inefficient ball mill. Also the overflow size ($x_{P,80}$) is influenced by hydrocyclone feed rate and feed pulp density.

The growth of the feed rate increases the centrifugal force effect which causes finer

particles being carried to the underflow, and hence decreasing the cut size. Further, the sharpness of separation decreases with increasing pulp density and the separation size rises due to higher resistance to swirling motion within the cyclone which reduces the effective pressure drop (Wills *et al*., 2006). In addition, feed rates for survey 1 and 2 were 10 and 18 % higher than design capacity of 1462 t/h, implying that hydrocyclones were overloaded.

Table 10: Ball mill performance indicators.

Parameter	S-1	S-2	S-3	Design
Ball mill feed $x_{F,80}$ (mm)	0. 963	1.028	1.127	
Ball mill discharge $x_{P,80}$ (mm)	0.570	0.419	0.403	0.125
Ball mill reduction ratio (-)	1.70	2.45	2.80	
Ball mill specific energy (kWh/t)	4.77	5.74	10.73	
Ball load, % volume	33	33	-	30-35

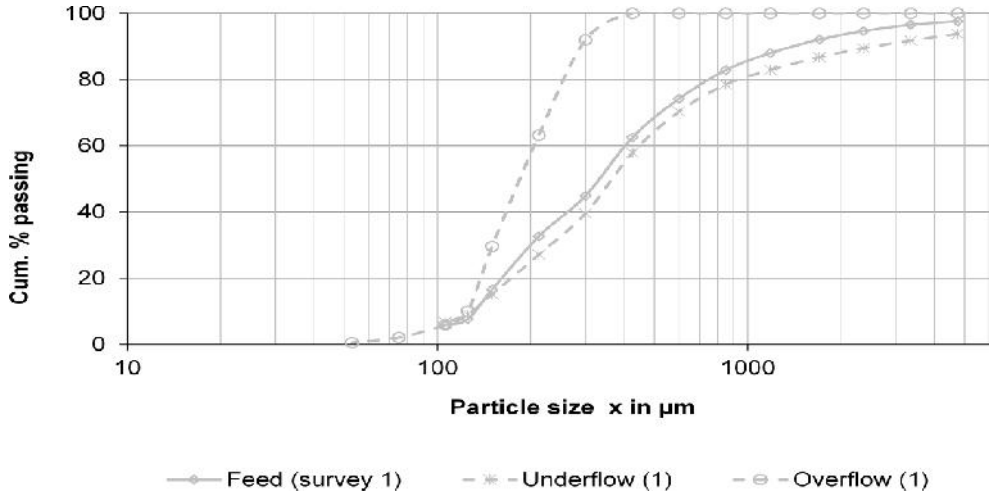

Figure 8: **Hydrocyclone product streams particle size distribution for survey 1**

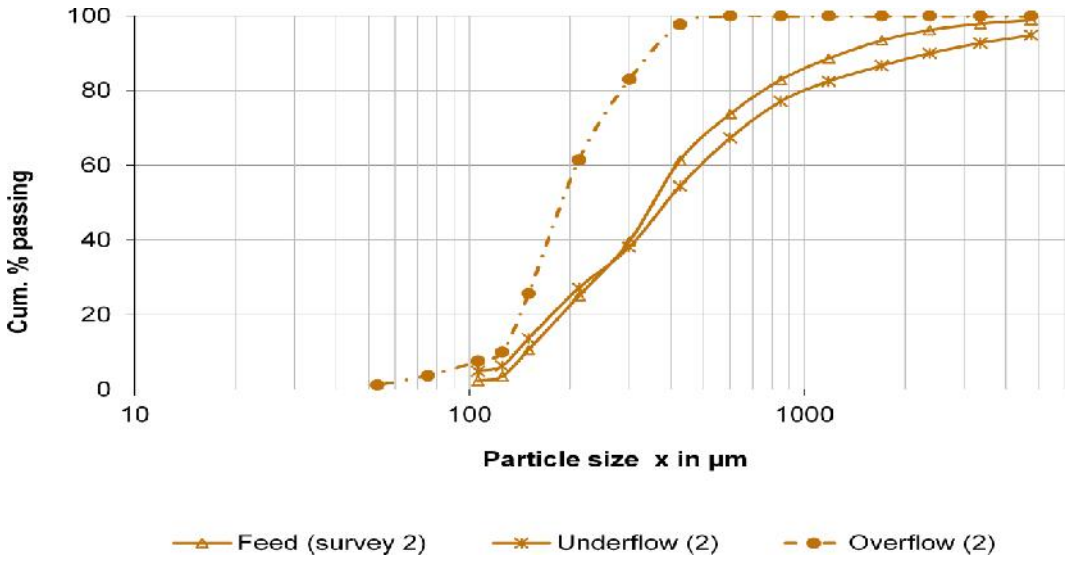

Figure 9: **Hydrocyclone product streams particle size distribution for survey 2**

Table 11: Hydrocyclone performance indicators.

Parameter	S-1	S-2	S-3	Design
Feed rate (t/h)	1729	1614	1061	1462
Operating pressure (kPa)	98	81	92	80-110
Feed volume-% solids	42	44	41	33
Underflow volume-% solids	57	57	56	48-56
Overflow volume-% solids	20	24	21	13-16
Feed $x_{P,80}$ (µm)	768	771	570	
Underflow $x_{P,80}$ (µm)	963	1028	1127	
Overflow $x_{P,80}$ (µm)	266	288	241	125

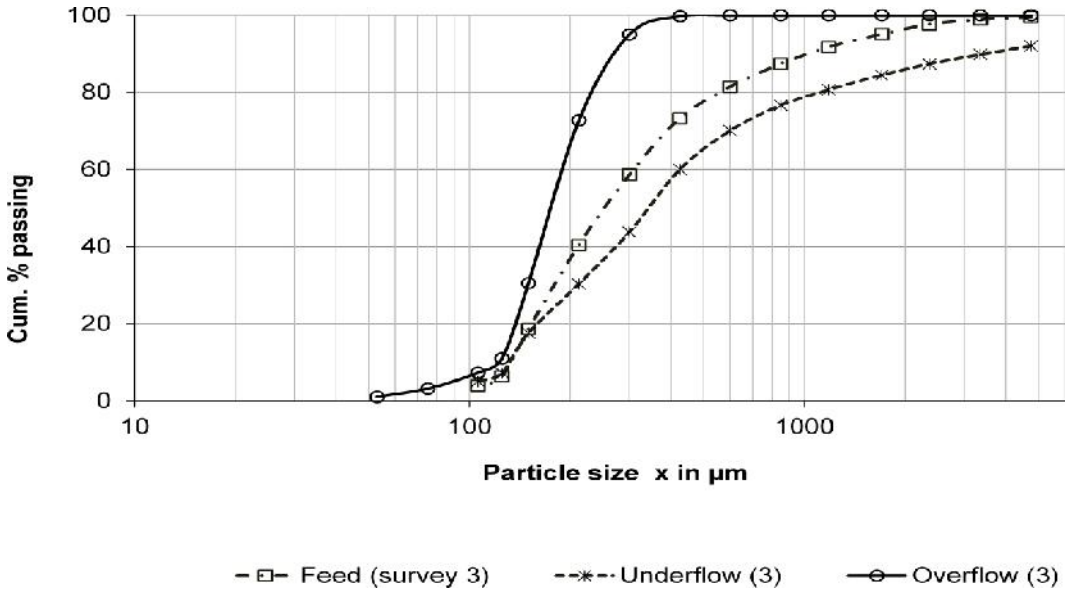

Figure 10: **Hydrocyclone product streams particle size distribution for survey 3**

The results of hydrocyclone efficiency for the BGM operation based on partition curves are shown in Figure 11. It can be observed that the by-pass fraction (split) was higher than 50 % and the cut size was higher than 200 µm for all three cases. This may also be related to the higher overflow $x_{P,80}$ obtained; clearly indicating that the current BGM operation is not able to achieve the target overflow size of 125 µm. The cut size and the by-pass fraction are influenced by feed pulp density and feed rate (Table 9). This is conforming with previous studies (Rybinski *et al*., 2011; Wills *et al*., 2006). In all of the three surveys, the hydrocyclone feed volume-% solids was 17 % higher than design (33 %v/v) and also higher than recommended values from literature (60 % solids or 35 % v/v). This is suspected to have contributed to the poor separation efficiency observed.

Nevertheless, the separation efficiency,=©= (Table 12) was fairly good for all surveys if the splitting effect was taken into account. The imperfection, *I*, can be used to categorize hydrocyclones (Guru and Basavaraj, 2012). Consequently, the hydrocyclones at BGM could be categorized (Table 13) between very good (i.e. $0.2 < I < 0.3$) and excellent (i.e. $I < 0.2$). This indicates that the current design is in principle fairly efficient for coarser overflow product and not for the current BGM target (i.e. $x_{P,80}$= 125 µm).

Therefore, the inefficiencies shown by the higher values of cut size could probably be an indication of the unsuitability of the

current design parameters for the target overflow of 125 µm. The influence of these design parameters on hydrocyclone cut size is clearly explained in literature (Schubert, 1985; Wills *et al*., 2006).

In practice, the selection of cut size is based on the designed size analysis of the overflow (Metso, 2010). For example, for BGM, the target overflow size amounts to $x_{P,80}$ = 125 µm, then the recommended cut size for efficient operation is 132.50 µm (obtained by multiplying target overflow size by the corresponding factor) in Table 14.

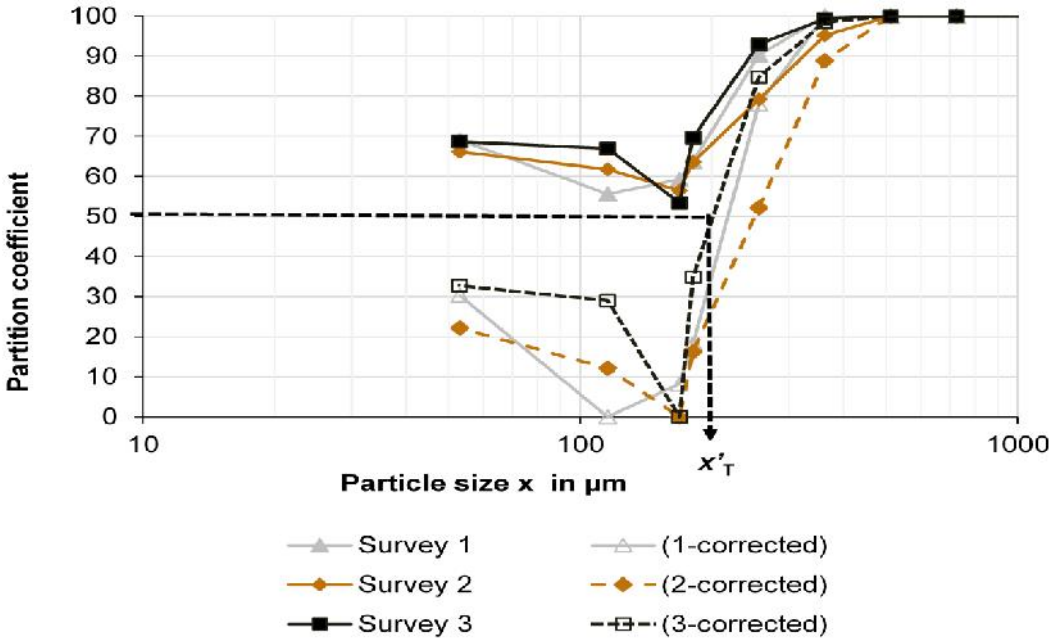

Figure 11: Hydrocyclone uncorrected and corrected efficiency curves for survey 1, 2 and 3

Table 12: Hydrocyclone efficiency indicators.

Parameter	S-1	S-2	S-3	Design
By-pass fraction (%)	55.60	56.00	53.42	
Cut size, x_T (µm)	220.84	251.45	203.75	
Imperfection, *I*	0.14	0.24	0.16	
Sharpness Index, ©	0.75	0.62	0.74	
Overflow $x_{P,80}$ (µm)	266	288	241	125

Table 13: Hydrocyclone efficiency category based on imperfection, I.

Imperfection, *I*- values	Separator category
< 0.2	Excellent separator
0.2 < *I* < 0.3	Very good separator
0.3 < *I* < 0.4	Medium separator
0.4 < *I* < 0.6	Poor separator
I > 0.6	Bad separator

Table 14: Factors for conversion of % passing in the overflow to X_T.

% passing in the overflow	99	95	90	80	70	60	50
Factor	0.49	0.65	0.79	1.06	1.36	1.77	2.34

Grinding Circuit Efficiency

Table 15 summarize the energy efficiency characteristic for the BGM operation. As seen in Table 15, the operating work index is more than twice the laboratory work index for each of the three surveys. This implies that, the circuit consumes more energy than the laboratory Bond test estimate and hence does not conform to the Bond standards in terms of energy efficiency (Alamouti *et al.*, 2011; Rowland, 2008). This can further be revealed by very low Bond efficiency factors (i.e. measure of the relative efficiency of the circuit compared to the prescribed Bond standard energy)of less than 65 %. Therefore, the operation is inefficient and could be optimized through decreased throughput.

The energy efficiency data (Table 16) reveal two options for the current BGM operation to achieve the target product size of 125 µm. A significant decrease in throughput by up to 44 % or an increase in input energy by up to 80 % (e.g. survey 1) are required in order to achieve such an improvement. The increase in input energy might be caused by the change in ore hardness. An increase in input energy requirement is not possible with the existing equipment, as this is equivalent to approximately 19 MW as opposed to the existing equipment capacity of 12 MW.

Table 15: **Energy consumption and operating work index for the current BGM operation**.

Parameter	Survey			Design
	S-1	S-2	S-3	
Throughput (t/h)	618.72	674.11	573.35	543-566
Circuit power (kW)	10,681	11,546	11,428	12,000
Input Energy (kWh/t)	17.26	17.13	19.93	
Operating W_i, (kWh/t)	35.62	30.78	34.91	
W_i (kWh/t)	17.2	18.70	18.50	14.5 -16.5
Bond efficiency, E (%)	48.30	60.70	52.90	

Table 16: Input energy and throughput required for the current operation to achieve $x_{P,80}$ of 125 µm

Survey	$x_{F,80}$ in mm	$x_{P,80}$ in µm	Throughput in t/h (compared to actual throughput)	Input energy in kWh/t
1	185	125	344 (-44.40 %)	31.03
2	102		435 (-35.50 %)	26.56
3	122		378 (-34.10 %)	30.22

CONCLUSIONS

Three full scale sampling campaigns and laboratory experimentation were conducted to evaluate the performance of BGM grinding circuit. The work index of the Buzwagi gold ore during plant design ranged from 14.5 to 16.5 kWh/t. The values obtained during the survey ranged between 17.20 - 18.70 kWh/t. This

indicates a change in the hardness of the ore during the last 7 years. Thus, a periodic review is required to assess the variation in hardness as mining progresses. This will help in establishing better blends and also predicting an appropriate tonnage for existing ore types, so as to be efficiently treated by existing capacity.

The comminution efficiency was determined using the Bond efficiency factor. Bond efficiency factors of 48-61 % were obtained for the BGM grinding operation, implying that the operation was inefficient and could probably achieve targets through reduced throughput. The SAG mill feed particle size distribution between the three surveys showed significant fluctuations ($x_{F,80}$: 102-185 mm). Since SAG mills use ore as part of the grinding media, regular monitoring and control of the ore feed size distribution is recommended as the change in feed size distribution normally results to corresponding changes in the grinding media size distribution, which has further impact on power and throughput. This could be fixed through closer monitoring of the primary crusher performance and also control of the ratios of SAG mill feeders which draws the ore from the stockpile.

The assessment of survey data indicated that the inefficiency of the ball mill was contributed by inefficient hydrocyclones. Apart from running at approximately 17 % above the design, hydrocyclones were also characterized by higher feed pulp densities (66.5-68.4%). In overall, this led to an overload of the ball mill due to increased circulating load. Classification efficiency could be improved by dilution of the feed in order to lower the pulp density, which could also improve the overflow density (i.e. closer to 30%) and hence giving a sharper cut.

Hence, an optimization study by computer simulation is further recommended. Through simulation of multi-effects, a deeper understanding of the efficiency problems for the BGM grinding operation will be facilitated and also may provide possible solutions. As the operations at BGM are close to an end, the findings from this study could be useful to other mining operations with similar problem.

ACKNOWLEDGEMENTS

The author would like to thank Buzwagi Gold Mine for allowing sampling at their plant as well as transportation of ore material to Germany for more test works. The Institute of Mechanical Process Engineering and Mineral Processing, TU Bergakademie Freiberg is also acknowledged for provision of laboratory facilities for the investigation.

REFERENCES

Acar C. (2013). Investigation of Particle Breakage Parameters in Locked-cycle Ball Milling. PhD Thesis, Middle East Technical University.

Alamouti B., Rezai B. and Noaparast M. (2011). Grinding Circuit at Mouteh Gold Mine. Amirkabir/MISC, 43(2): 71–76.

Ballantyne G., Powell M. and Tiang M. (2012). Proportion of Energy Attributable to Comminutione, in: 11th Mill Operators' Conference. Hobart.

Bond F.C. (1961). Crushing and grinding calculations, Part I-II. Br. Chem. Eng., 153: 362–373.

Bond F.C. (1952). The Third Theory of Comminution. Trans. AIME 193: 484–494.

Bond F.C. and Maxson W.L. (1943). Standard grindability tests and calculations. Transactions 153: 362–373.

Boucaut S. (2017). Energy in Mining. [WWW Document]. URL https://ceecthefuture.org/why-smart-companies-are-focusing-on-comminution/. (accessed on 11.28.20).

Curry J.A., Ismay M.J.L. and Jameson G.J. (2014). Mine operating costs and the potential impacts of energy and grinding. Miner. Eng. 56: 70–80. https://doi.org/10.1016/j.mineng.2013.10.020

Danha G. (2013). Identifying Opportunities for Increasing the Milling Efficiency of a Bushveld Igneous Complex (BIC) Upper Group (UG) 2 Ore. University of Witwatersrand, South Africa.

Denız V. (2011). Computer Simulation of Product Size Distribution of a Laboratory Ball Mill. Part. Sci. Technol. 29: 541–553. https://doi.org/10.1080/02726351.2010.536303

Fuerstenau D.W., Phatak P.B., Kapur P.C. and Abouzeid A.Z.M. (2011). Simulation of the grinding of coarse/fine (heterogeneous) systems in a ball mill. Int. J. Miner. Process., 99: 32–38. https://doi.org/10.1016/j.minpro.2011.02.003

Gupta A. and Yan D.S. (2006). Introduction to Mineral Processing Design and Operation. Perth, Australia.

Guru N.M. and Basavaraj K. (2012). Assessing the performance of a floatex density separator for the recovery of iron from low-grade australian iron ore fines – a case study, in: XXVI International Mineral Processing Congress (IMPC). New Delhi, India.

Jeswiet J. and Szekeres A. (2016). Energy Consumption in Mining Comminution. Procedia CIRP 48: 140–145. https://doi.org/10.1016/j.procir.2016.03.250

Khumalo N. (2007). The Application of the Attainable region analysis in Comminution. University of the Witwatersrand, South Africa.

Leißner T., Hoang D.H., Rudolph M., Heinig T., Bachmann K., Gutzmer J., Schubert H. and Peuker U.A. (2016). A mineral liberation study of grain boundary fracture based on measurements of the surface exposure after milling. Int. J. Miner. Process. 156: 3–13. https://doi.org/10.1016/j.minpro.2016.08.014

Magdalinović N. (1989). A procedure for rapid determination of the Bond work index. Int. J. Miner. Process. 27: 125–132. http://dx.doi.org/10.1016/0301-7516(89)90010-0

Man Y.T. (2002). Why is the Bond Ball Mill Grindability Testdone the way it is done? Eur. J. Miner. Process. Environ. Prot., 2: 34–39.

Masuda H., Higashitani K., Yoshinda H. (2007). Powder Technology: Handling and Operations, Process Instrumentation, and Working Hazards. Taylor and Francis, Boca Raton.

Metso (2010). Basics of mineral processing. Metso, Helsinki, Finland.

Mosher J.B. and Tague C.B. (2001). Conduct and precision of bond grindability testing. Miner. Eng., 14(10): 1187–1197. https://doi.org/10.1016/S0892-6875(01)00136-4

Mular A.L., Haibe D.N. and Barrett D.J. (2002). Mineral Processing Plant Design, Practice, and Control. SME.

Napier-Munn T.J., Morrel S. and Kojovic T. (1996). Mineral Comminution Circuits: Their Operation and Optimisation, JKMRC Monograph Series in Mining and Mineral Processing 2. JKMR, Queensland, Australia.

NRC (1981). Comminution and Energy Consumption. Washington DC.

Pourghahramani P. (2012). Effects of ore characteristics on product shape properties and breakage mechanisms in industrial SAG mills. Miner. Eng., 32: 30–37. https://doi.org/10.1016/j.mineng.2012.03.005

Rosario P.P. (2010). Comminution Circuit Design and Simulation for the Development of a Novel High Pressure Grinding Roll Circuit. University of

British Columbia.

Rowland C.A. (2008). The Standard for Comminution Efficiency, in: SME Annual Meeting. SME, Salt Lake City, Uhah, USA.

Rowland C.A. (2006). Bond's Method for Selection of Ball Mills, in: Advances in Comminution. SME, Littleton, Colorado, USA.

Rybinski E., Ghersi J., Davila F., Linares J., Valery W., Jankovic A., Valle R., and Dikmen S. (2011). Optimisation and continuous improvement of Antamina comminution circuit, in: SAG Conference. Vancouver, Canada.

Saramak D., Tumidajski T., Brożek M., Gawenda T. and Naziemiec Z. (2010). Aspects of comminution flowsheets design in processing of mineral raw materials. Gospod. Surowcami Miner., 26: 59–69.

Schlanz J.W. (1987). Grinding: An Overview of Operation and Design . Mill Oper. Symp.

Schubert H. (2003). "Zu den Ursachen 'anomaler' Verläufe der Trennkurve bei der Feinstkornklassierung in Hydrozyklonen – insbesondere zum so genannten Fish-Hook-Effekt*)." Aufbereit. Tech., 44: 5–17.

Schubert H. (1985). A hydrocyclone separation model in consideration of the turbulent multi-phase flow. Part. Sci. Technol., 3: 1–13. https://doi.org/10.1080/02726358508906423

Schubert H. and Mühle K. (1991). The role of turbulence in unit operations of particle technology. Adv. Powder Technol., 2: 295–306. https://doi.org/10.1016/S0921-8831(08)60696-2

Tromans D. (2008). Mineral comminution: Energy efficiency considerations. Miner. Eng., 21: 613–620. https://doi.org/10.1016/j.mineng.2007.12.003

Vedat D. (2011). Influence of interstitial filling on breakage kinetics of gypsum in ball mill. Adv. Powder Technol., 22: 512–517. http://dx.doi.org/10.1016/j.apt.2010.07.004

Wikedzi A. (2018). Optimization and Performance of Grinding Circuits: The Case of Buzwagi Gold Mine (BGM). TU Bergakademie Freibergy.

Wills B.A. and Finch J.A. (2016). Wills' Mineral Processing Technology: An Introduction to the Practical Aspects of Ore Treatment and Mineral Recovery. Elsevier, Oxford.

Wills B.A., Napier-Munn T. and Napier-Munn T. (2006). Wills' Mineral Processing Technology: An Introduction to the Practical Aspects of Ore Treatment and Mineral Recovery, 7th ed. Butterworth-Heinemann, Oxford.